

Seismic assessment of masonry structures by non-linear macro-element analysis

A. Penna

European Centre for Training and Research in Earthquake Engineering, Pavia, Italy

S. Cattari, A. Galasco & S. Lagomarsino

Department of Structural and Geotechnical Engineering, University of Genoa, Italy

ABSTRACT: Complete 3D models of existing masonry structures can be obtained assembling 2-nodes macro-elements, representing the non-linear behavior of masonry panels and piers. This modeling strategy has been implemented in the TREMURI program with non-linear static and dynamic analysis procedures requiring limited computational loads. By means of internal variables, the macro-element considers both the shear-sliding damage failure mode and its evolution, controlling the strength deterioration and the stiffness degradation, and rocking mechanisms, with toe crushing effect. Masonry building models can be obtained assembling plane structures, walls and floors.

1 INTRODUCTION

The need for masonry structure modeling and analysis tools is largely diffused worldwide. Very sophisticated finite element models or extremely simplified methods are commonly used for the seismic analysis of this kind of structures. In this paper, by means of the effective macro-element approach, an accurate, but without heavy computational load, modeling strategy is presented and developed for the analysis of both building and bridge structures.

Case studies and examples, both from experimental testing and earthquake damaged structures, show the modeling technique effectiveness and the seismic analysis capabilities. Pushover analyses provide capacity curves and equivalent hysteretic damping evaluation: these results permit to assess the applicability of the Capacity Spectrum Method to masonry structures, checking the seismic performance prediction by dynamic analyses.

2 STRUCTURAL MODEL

2.1 Non-linear macro-element model

The non-linear macro-element model, representative of a whole masonry panel, proposed by Gambarotta and Lagomarsino (1996), permits, with a limited number of degrees of freedom (8), to represent the two main in-plane masonry failure modes, bending-rocking and shear-sliding (with friction) mechanisms, on the basis of mechanical assumptions. This model considers, by means of internal variables, the shear-sliding damage evolution, which controls the strength

deterioration (softening) and the stiffness degradation.

Figure 1 shows the three sub-structures in which a macro element is divided: two layers, inferior ① and superior ③, in which the bending and axial effects are concentrated. Finally, the central part ② suffers shear-deformations and presents no evidence of axial or bending deformations. A complete 2D kinematic model should take into account the three degrees of freedom for each node "i" and "j" on the extremities: axial displacement w , horizontal displacement u and rotation j . There are two degrees of freedom for the central zone: axial displacement d and rotation f (Figure 1).

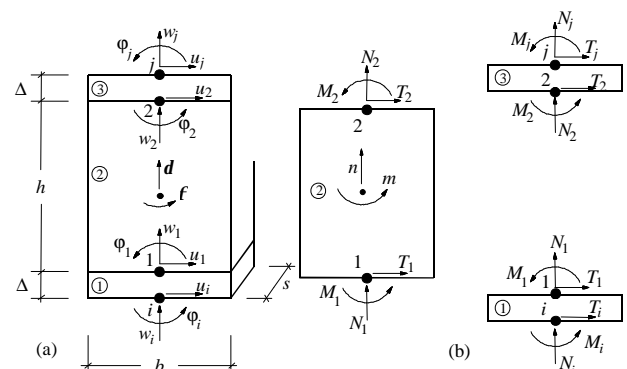


Figure 1. Kinematic model for the macro-element

Thus, the kinematics is described by an eight degree freedom vector, $a^T = \{u_i \ w_i \ \phi_i \ u_j \ w_j \ \phi_j \ \delta \ \phi\}$, which is obtained for each macro-element. It is assumed that the extremities have an infinitesimal thickness ($\Delta \rightarrow 0$).

The overturning mechanism, which happens because the material does not show tensile strength,

is modeled by a mono-lateral elastic contact between ① and ③ interfaces. The constitutive equations between the kinematic variables w , \mathbf{j} and the correspondent static quantities $\frac{m}{n}$ and m are uncoupled until the limit condition $\left|\frac{m}{n}\right| \leq \frac{6}{b}$, for which the partialization effect begins to develop in the section.

For sub-structure ① the following equations are obtained:

$$N_i = kA(\mathbf{d} - w_i) + N_i^* \quad (1)$$

$$M_i = \frac{1}{12}kAb^2(\mathbf{j}_i - \mathbf{f}) + M_i^* \quad (2)$$

where $A = s \cdot b$ corresponds to the transversal area of the panel. The inelastic contribution N_i^* and M_i^* are obtained from the mono-lateral condition of perfect elastic contact:

$$N_i^* = \frac{-k \cdot A}{8|\mathbf{j}_i - \mathbf{f}|} [|\mathbf{j}_i - \mathbf{f}|b + 2(\mathbf{d} - w_i)]^2 H\left(|e_i| - \frac{1}{6}b\right) \quad (3)$$

$$M_i^* = \frac{k \cdot A}{24(\varphi_i - \phi_i)} [(\varphi_i - \phi_i)b - (\delta - w_i)] [|\varphi_i - \phi_i|b + 2(\delta - w_i)]^2 H\left(|e_i| - \frac{1}{6}b\right) \quad (4)$$

where $H(\bullet)$ is the Heaviside function.

The panel shear response is expressed considering a uniform shear deformation distribution

$\mathbf{g} = \frac{u_i - u_j}{h} + \mathbf{f}$ in the central part ② and imposing a

relationship between the kinematic quantities u_i , u_j and \mathbf{f} , and the shear stress $T_i = -T_j$. The cracking damage is usually located on the diagonal, where the displacement take place along the joints and is represented by an inelastic deformation component, which is activated when the Coulomb's limit friction condition is reached. From the effective shear deformation corresponding to module ② and indicating the elastic shear module as G , the constitutive equations can be expressed as:

$$T_i = \frac{GA}{h}(u_i - u_j + \mathbf{f}h) + T_i^* \quad (5)$$

$$T_i^* = -\frac{GA}{h} \frac{c\mathbf{a}}{1+c\mathbf{a}} \left(u_i - u_j + \mathbf{f}h + \frac{h}{GA} f \right) \quad (6)$$

where the inelastic component T_i^* includes the friction stress f effect, opposed to the sliding mechanism, and involves a damage parameter \mathbf{a} and a non-dimensional coefficient c , that controls the inelastic deformation. In this model, the friction plays the role of an internal variable, defined by the following limit condition:

$$\Phi_S = |f| - \mathbf{m} \cdot N_i \leq 0, \quad (7)$$

where \mathbf{m} corresponds to the friction coefficient. These constitutive equations can represent the panel

resistance variation due to changes on axial stresses $N_j = -N_i$. The damage effects upon panel mechanical characteristics are described by the damage variable \mathbf{a} , that grows according to a pre-defined failure criteria:

$$\Phi_d = Y(S) - R(\mathbf{a}) \leq 0, \quad (8)$$

where $Y = \frac{1}{2}cq^2$ is the damage energy release rate; R is the resistance function and $S = \{t \ n \ m\}^T$ is the internal stress vector. Assuming R as a growing function of \mathbf{a} to the critical value $\mathbf{a}_C = 1$ and decreasing for higher values, the model can represent the stiffness degradation, the strength degradation and pinching effect.

The complete constitutive model, for the macro element, can be expressed in the following form:

$$Q = Ka + Q^* \quad (9)$$

where $Q^* = \{T_i^* \ N_i^* \ M_i^* \ T_j^* \ N_j^* \ M_j^* \ N^* \ M^*\}$ contains the non-linear terms evaluated by the evolution equations, related to the damage variable \mathbf{a} and the friction f , and K is the elastic stiffness matrix.

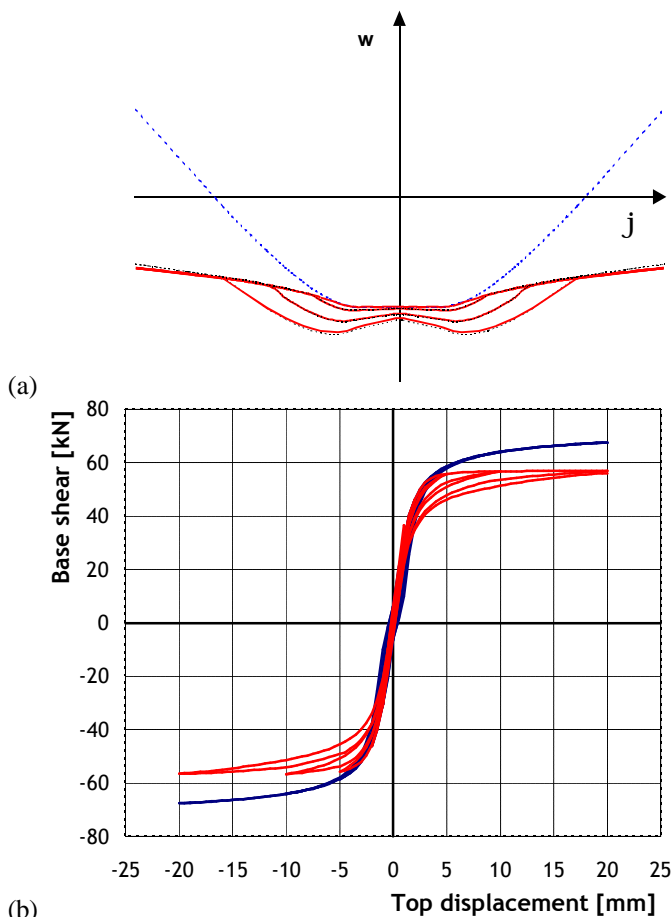
The non-linear terms N^* and M^* are defined through the following equation:

$$N^* = N_j^* - N_i^*; M^* = -M_j^* - M_i^* + T_i^* h \quad (10)$$

The macro-element shear model is a macroscopic representation of a continuous model (Gambarotta & Lagomarsino 1997), in which the parameters are directly correlated to the mechanical properties of the masonry elements. The macro-element parameters should be considered as representative of an average behaviour. In addition to its geometrical characteristics, the macro-element is defined by six parameters: the shear module G , the axial stiffness K , the shear strength f_{vq0} of the masonry, the non-dimensional coefficient c that controls the inelastic deformation, the global friction coefficient f and the \mathbf{b} factor, that controls the softening phase.

2.2 Toe crushing and compressive damage model

The macro-element used in the program to assemble the wall model keeps also into account the effect (especially in bending-rocking mechanisms) of the limited compressive strength of masonry (Penna 2002). Toe crushing effect is modelled by means of phenomenological non-linear constitutive law with stiffness deterioration in compression: the effect of this modellization on the cyclic vertical displacement-rotation interaction is represented in Figure 2.



(b) Figure 2. (a) Cyclic vertical displacement-rotation interaction with (line) and w/o toe crushing (dots) (Penna, 2002); (b) Rocking panel with and without crushing.

2.3 3D MASONRY BUILDING MODEL

The 3-dimensional modelling of whole URM buildings starts from some hypotheses on their structural and seismic behaviour: the bearing structure, both referring to vertical and horizontal loads, is identified, inside the construction, with walls and floors (or vaults); the walls are the bearing elements, while the floors, apart from sharing vertical loads to the walls, are considered as planar stiffening elements (orthotropic 3-4 nodes membrane elements), on which the horizontal actions distribution between the walls depends; the local flexural behaviour of the floors and the walls out-of-plane response are not computed because they are considered negligible with respect to the global building response, which is governed by their in-plane behaviour (a global seismic response is possible only if vertical and horizontal elements are properly connected).

A frame-type representation of the in-plane behaviour of masonry walls is adopted: each wall of the building is subdivided into piers and lintels (2 nodes macro-elements) connected by rigid areas (nodes) (see Figure 4). Earthquake damage observation shows, in fact, that only rarely (very irregular geometry or very small openings) cracks appear in these areas of the wall: because of this, the

deformation of these regions is assumed to be negligible, relatively to the macro-element non-linear deformations governing the seismic response. The presence of stringcourses (beam elements), tie-rods (non-compressive spar elements), previous damage, heterogeneous masonry portions, gaps and irregularities can be easily included in the structural model.

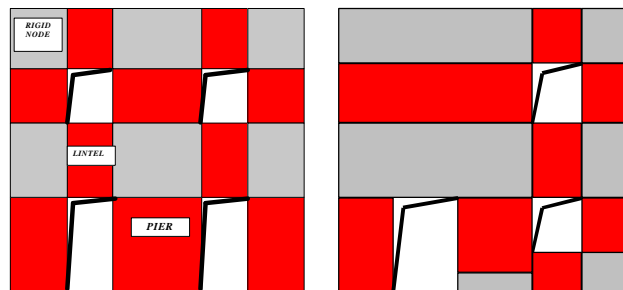


Figure 3. Macro-element modelling of masonry walls.

The non-linear macro-element model, representative of a whole masonry panel, is adopted for the 2-nodes elements representing piers and lintels. Rigid end offsets are used to transfer static and kinematic variables between element ends and nodes.

A global Cartesian coordinate system (X,Y,Z) is defined and the wall vertical planes are identified by the coordinates of one point and the angle formed with X axis. In this way, the walls can be modelled as planar frames in the local coordinate system and internal nodes can still be 2-dimensional nodes with 3 d.o.f..

The 3D nodes connecting different walls in corners and intersections need to have 5 d.o.f. in the global coordinate system $(u_x, u_y, u_z, rot_x, rot_y)$: the rotational degree of freedom around vertical Z axis can be neglected because of the membrane behaviour adopted for walls and floors. These nodes can be obtained assembling 2D rigid nodes acting in each wall plane (see Figure 4) and projecting the local degrees of freedom along global axes.

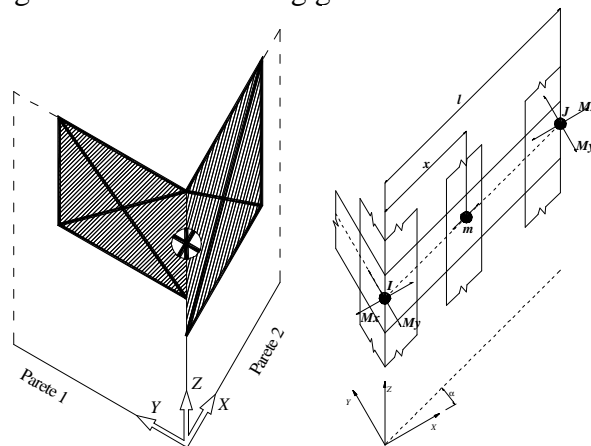


Figure 4. Scheme of 3D and 2D nodes and out-of-plane mass sharing.

The floor elements, modelled as orthotropic membrane finite elements, with 3 or 4 nodes, are

identified by a principal direction, with Young modulus E_1 , while E_2 is the Young modulus along the perpendicular direction, ν is the Poisson ratio and $G_{1,2}$ the shear modulus: E_1 and E_2 represent the wall connection degree due to the floors, by means also of stringcourses and tie-rods. $G_{1,2}$ represents the in-plane floor shear stiffness which governs the horizontal actions repartition between different walls.

Having the 2D nodes no degrees of freedom along the orthogonal direction to the wall plane, in the calculation the nodal mass component related to out-of-plane degrees of freedom is shared to the corresponding dofs of the nearest 3D nodes of the same wall and floor according to the following relations:

$$\begin{aligned} M_x^I &= M_x^I + m(1 - |\cos \mathbf{a}|) \frac{l-x}{l}, \\ M_y^I &= M_y^I + m(1 - |\sin \mathbf{a}|) \frac{l-x}{l} \end{aligned} \quad (11)$$

where the meaning of the terms is shown in Figure 4.

This solution then permits the implementation of static analyses with 3 components of acceleration along the 3 principal directions and 3D dynamic analyses with 3 simultaneous input components, too.

3 SEISMIC ANALYSIS PROCEDURES

In order to perform non-linear seismic analyses of masonry buildings a set of analysis procedures has been implemented (Galasco *et al.*, 2002): incremental static (Newton-Raphson) with force or displacement control, 3D pushover analysis with fixed load pattern and 3D time-history dynamic analysis (Newmark integration method; Rayleigh viscous damping), considering uniform or spatially varying motion. The pushover procedure, with an effective algorithm, transforms the problem of pushing a structure maintaining constant ratios between the applied forces into an equivalent incremental static analysis with one d.o.f. displacement response control.

3.1 Pushover analysis

The general formulation of the pushover problem can be represented by equations:

$$\begin{bmatrix} \mathbf{K}_{FF} & \mathbf{k}_{Fm} & \mathbf{K}_{FC} \\ \mathbf{k}_{Fm}^T & k_{mm} & \mathbf{k}_{Cm}^T \\ \mathbf{K}_{CF} & \mathbf{K}_{Cm} & \mathbf{K}_{CC} \end{bmatrix} \begin{Bmatrix} \mathbf{x}_F \\ x_m \\ \mathbf{x}_C \end{Bmatrix} = \begin{Bmatrix} \mathbf{I} \mathbf{f}_F \\ \mathbf{I} f_m \\ \mathbf{r}_C \end{Bmatrix}, \quad (12)$$

where m is the control degree of freedom and \mathbf{f}_F is the applied load pattern coefficient vector.

The system of equations can be transformed subtracting the m -th row from the first $m-1$, the i -th equation then becomes:

$$\left(k_{i1} - \frac{f_i}{f_m} k_{m1} \right) x_1 + \dots + \left(k_{im} - \frac{f_i}{f_m} k_{mm} \right) x_m + \dots + \left(k_{in} - \frac{f_i}{f_m} k_{nn} \right) x_n = 0. \quad (13)$$

The new system of equations, with a modified stiffness matrix,

$$\begin{bmatrix} \tilde{\mathbf{K}}_{FF} & \tilde{\mathbf{k}}_{Fm} & \tilde{\mathbf{K}}_{FC} \\ \mathbf{k}_{Fm}^T & k_{mm} & \mathbf{k}_{Cm}^T \\ \mathbf{K}_{CF} & \mathbf{K}_{Cm} & \mathbf{K}_{CC} \end{bmatrix} \begin{Bmatrix} \mathbf{x}_F \\ x_m \\ \mathbf{x}_C \end{Bmatrix} = \begin{Bmatrix} \mathbf{0} \\ \mathbf{I} f_m \\ \mathbf{r}_C \end{Bmatrix}, \quad (14)$$

is then equivalent to a displacement control one, in which the m -th d.o.f. (x_m) is the imposed one. This formulation can be easily rewritten by introducing the non-linear contribution and in incremental form, in order to be implemented in the non-linear procedure.

4 EXPERIMENTAL TEST AND EARTHQUAKE DAMAGE SIMULATION

4.1 University of Pavia quasi-static tests

In order to demonstrate the reliability of the model, a numerical simulation of experimental testing on a full-scale masonry building accomplished in the Laboratory of the University of Pavia (Magenes & Calvi, 1997) is here presented.

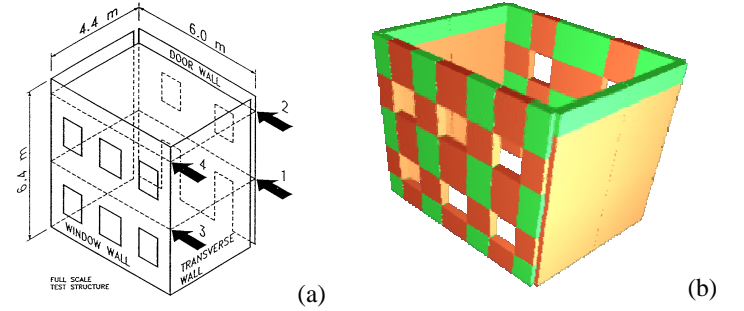


Figure 5. (a) Scheme of the test; (b) 3-dimensional view of the macro-element model.

As shown in Figure 5-a, the experimental tests have been carried out on two separated structural systems: the isolated “door” wall and the “window” wall connected to the two transverse walls. The numerical simulation has then performed by cyclic analysis of two different macro-element models (Figure 6) with the same mechanical characteristics: the window wall system has been modelled using 12 nodes and 21 macro-elements, the door wall 9 nodes and 10 macro-elements.

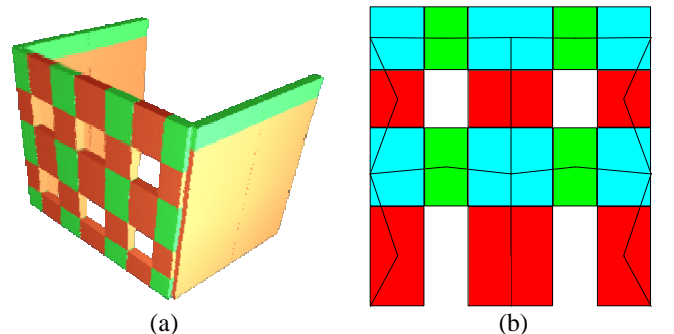


Figure 6. (a) 3D model of window and transverse walls; (b) 2D model of door wall.

The numerical and experimental results are in good accordance, both in terms of cyclic base shear-second floor displacement curves (Figures 7,8) and damage localization at the different load steps. The model can well represent the real collapse mechanism and reproduce correct levels of strength and hysteretic energy dissipation.

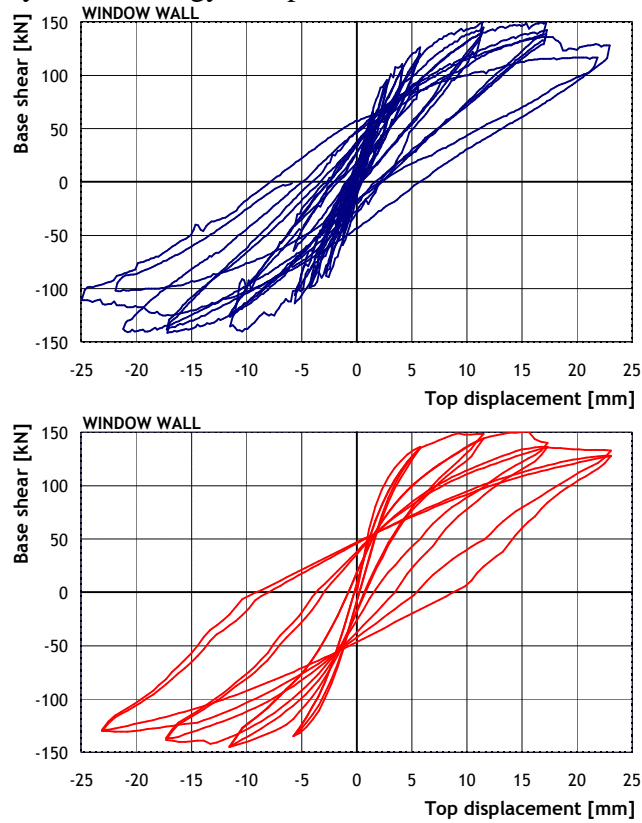


Figure 7. Comparison of experimental (top) and numerical results (window wall).

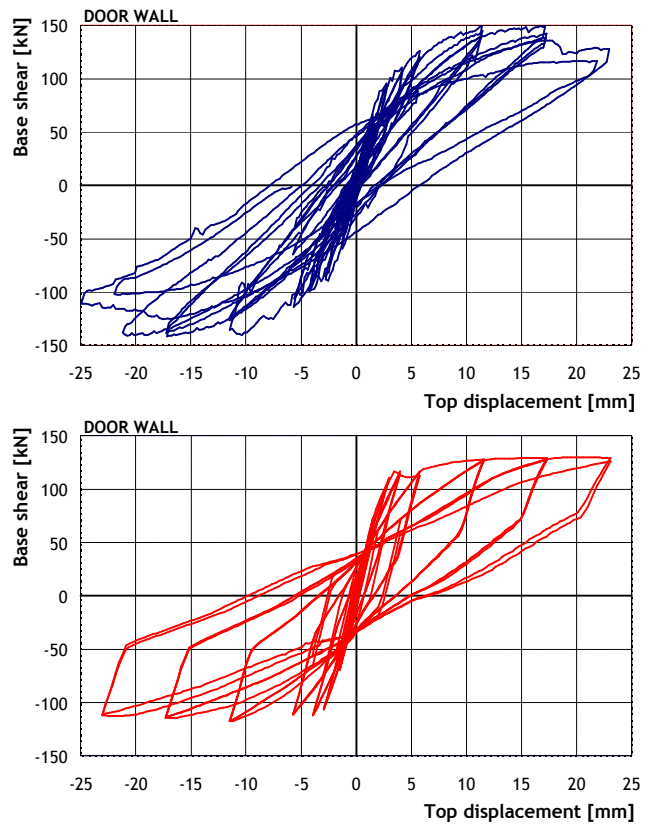


Figure 8. Comparison of experimental (top) and numerical results (door wall).

4.2 Earthquake damage

A complete 3D macro-element model (Figure 9) of the Hall of Castelnuovo Belbo village, in Piedmont, Northern Italy, has been used in order to simulate the building seismic response and the damage pattern surveyed after August 21st 2000 Monferrato earthquake ($M_d=4.6$).

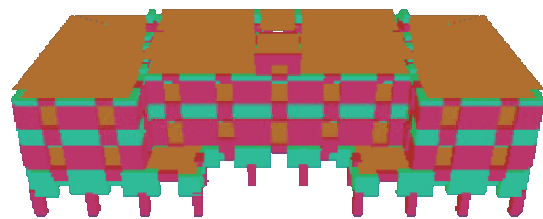


Figure 9. Aerial view of the building and perspective view of TREMURI 3D model.

By means of a non-linear time-history analysis, the global seismic response has been investigated: an artificial accelerogram scaled to the maximum recorded PGA during the seismic event (0.14 g) has been used as input.

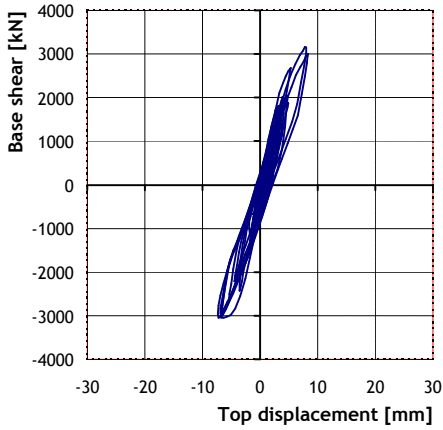


Figure 10. Dynamic force-displacement response and damage pattern in a wall.

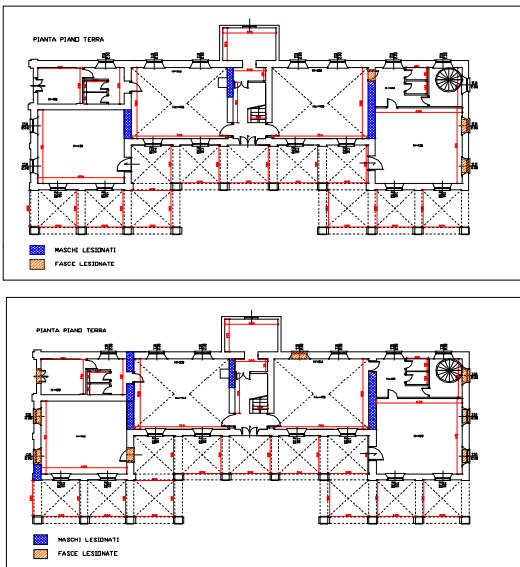


Figure 11. Damage pattern simulation: surveyed (top) and simulated damage at the ground floor.

5 CASE STUDY: A TYPICAL BUILDING OF THE EIXAMPLE DISTRICT IN BARCELONA

A significant application of the proposed modeling strategy has been performed by Bonett *et al.* (2003) on a typical building in Barcelona, Spain within the RISK-UE Project: Figure 12 shows a three-dimensional view and in plan of the model used for the prototype building representative of the very particular structural typology of the Eixample district. The model is defined by 8 walls in the x

direction (walls M1 to M8) and 6 walls in the y direction (walls M9 to M14). Each wall has been modeled as an assemblage of piers, lintels and frame elements (in some cases) connected to the nodes of the model by means of rigid joints. The slabs have been modeled as an orthotropic finite elements diaphragm, defined by 3 or 4 nodes connected to the three-dimensional nodes of each level. A main direction is identified, which is characterized by a Young's modulus E_1 and the direction perpendicular to this one is characterized by a Young's modulus E_2 . Figure 15 shows the macro element model corresponding to walls 1 and 2.

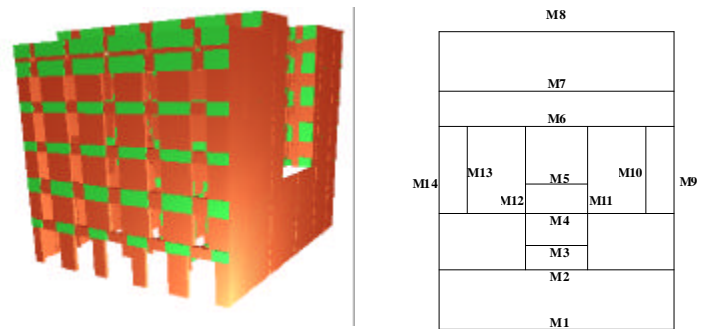


Figure 12. Three-dimensional model of the analyzed typical building of the Eixample.

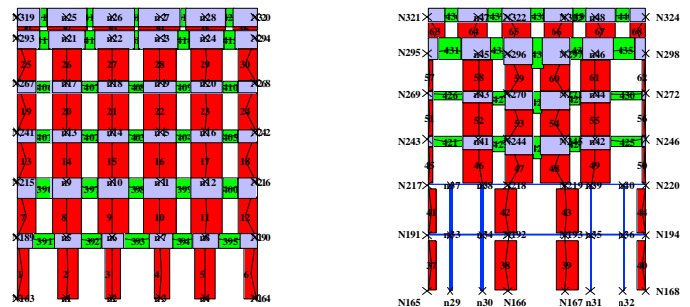


Figure 13. Macro element model for walls 1 and 2.

In order to analyze the constructive system of the URM buildings of the Eixample, it is necessary to have a good knowledge on the materials used in building their main elements. The bricks are the basic material of these buildings, being used widely in walls, stairs and slabs. The typical dimensions of the used bricks are of 30 cm \times 15 cm and with thicknesses varying between 3 cm and 11 cm and were until the beginning of the XXth century. Later, mechanical systems were used, what improved considerably their compactness. Lime mortar was used in the constructive process of the buildings of the Eixample. The wide use of this material is associated to constructive tradition, to consumption habits and, apparently, to its strength which was considering adequate at that period.

In this work, probability distribution functions, *pdf*, are used to define the most important parameters of the model. These functions are characterized by a mean value and a covariance. The

definition of the mean value of each parameter has been defined using the opinion of experts, who provided sufficient information for defining a model. Nevertheless, due to the subjective character of this information, the main parameters have been considered as random variables with their uncertainties. The most important mechanical properties of the materials used in the analysis of the building of the Eixample are described below.

Masonry

Young's modulus of the wall $E = 2.10 \cdot 10^9 \text{ N/m}^2$

Shear modulus $G = 0.7 \cdot 10^9 \text{ N/m}^2$

Shear strength $\tau = 1.0 \cdot 10^5 \text{ N/m}^2$

Softening factor for the piers $\beta_p = 0.5$

Softening factor for the lintels $\beta_d = 0.05$

Cast iron columns

Young's modulus $E_s = 2.10 \cdot 10^{11} \text{ N/m}^2$

Specific weight $\gamma_s = 7850 \text{ kg/m}^3$

Concrete columns

Young's modulus $E_h = 2.8 \cdot 10^9 \text{ N/m}^2$

Specific weight $\gamma_h = 2500 \text{ kg/m}^3$

Slabs

Young's modulus (main direction) $E_1 = 4.20 \cdot 10^9 \text{ N/m}^2$

Young's modulus (orthogonal direction) $E_2 = 4.20 \cdot 10^7 \text{ N/m}^2$

Shear modulus $G = 0.4 \cdot 10^9 \text{ N/m}^2$

Among all these characteristics, those shown in Table 1 have been defined as random variables because they have an important influence on the structural response of this one type of buildings. The normal probability distribution function has been used for the three variables, where the mean value of each parameter corresponds to the values proposed by experts. The covariance has been defined in such a way to cover the range of the possible values of each parameter.

Table 1. Probability distribution functions, median values and covariance of the random variables.

Parameter	PDF	Mean	Covariance
Young's modulus E	normal	$2.1 \cdot 10^9 \text{ Pa}$	0.3
Shear strength τ	normal	$1.0 \cdot 10^5 \text{ Pa}$	0.3
Softening factor β_p	normal	0.5	0.3

5.1 Capacity curve

The capacity curve is obtained applying a force distribution pattern corresponding to the bending modal shape oriented along the y axis.

This curve describes the relationship between base shear and the roof displacement of an equivalent single degree of freedom model. The response of the model of the typical URM building is defined by means of the capacity curves obtained by means of the Monte Carlo simulation technique. Thus, 100 samples for each variable were generated and a structural model was defined for each sample group. One hundred capacity curves were thus obtained.

The advanced computational tool STAC (2002) has been used in the simulation process. Figure 14 shows to the capacity spectra corresponding to the mean value and to the corresponding standard deviations. This type of the representation shows the sensitivity of these analysis methods to the uncertainties in the structural parameters.

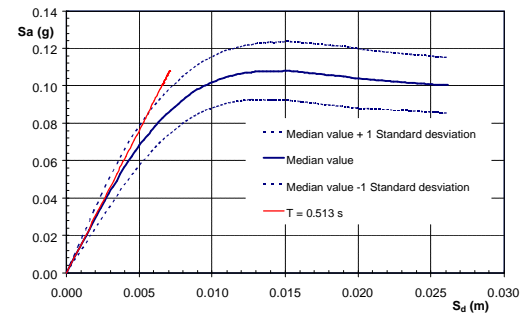


Figure 14. Median, median + 1σ , median - 1σ capacity spectra.

5.2 Damage states

In order to obtain the damage states limits or the performance levels of the URM building of the Eixample, there are neither laboratory tests nor available values calibrated from the observed damages during earthquakes. Additionally, the values of the mechanical properties of the materials used in this structural typology are not completely known. Taking into account all these aspects, the thresholds of the spectral displacement for the discrete damage states are defined based on the bilinear simplification of the capacity spectrum.

A possible definition the thresholds of the spectral displacement for four damage states is shown in table 2.

Table 2. Displacement limit states

Damage state	Spectral displacement threshold
Slight	$0.7D_y^*$
Moderate	D_y^*
Extensive	$D_y^* + 0.25(D_u^* - D_y^*)$
Complete	D_u^*

* D_y^* and D_u^* are respectively the equivalent yielding and ultimate displacement of the bilinear capacity spectrum

5.3 Seismic performance assessment

In order to evaluate the seismic performance of the typical masonry building of the Eixample, the N2 method proposed by Fajfar (1999) was adopted. The seismic input, described by acceleration-displacement response spectra, was spatially varied along the district and the expected damage states were mostly between slight and moderate (operational and life-safe).

6 CONCLUSIONS

As shown in the paper, the non-linear macro-element modelling of 3-dimensional masonry buildings supplies reliable results in comparison with experimental data and permits to model effectively different typologies of real masonry structures, too. Its seismic analysis capabilities make the TREMURI program a valid tool both for research activity and engineering practice, especially regarding the safety assessment of existing masonry buildings. The macro-element model permits to perform reliable non-linear seismic analyses of wide masonry structures with a limited number of d.o.f. and relatively short analysis time using common PC technology. Modern performance-based seismic engineering requires this kind of easy-to-use tools for both capacity assessment and direct time-history response evaluation.

The assessed seismic performances of a masonry building, typical for the Eixample area of Barcelona, show high vulnerability and possible damage due to relatively small earthquakes.

REFERENCES

1. Gambarotta L., Lagomarsino S., 1996, "On dynamic response of masonry panels", in Gambarotta L. (ed.) Proc. Nat. Conf. "Masonry mechanics between theory and practice", Messina, (in italian).
2. Gambarotta L., Lagomarsino S., 1997, "Damage models for the seismic response of brick masonry shear walls, Part II: the continuum model and its applications", Earth. Engineering and Structural Dynamics, 26.
3. Penna A., 2002, "A macro-element procedure for the non-linear dynamic analysis of masonry buildings", Ph.D. Dissertation (in italian), Politecnico di Milano, Italy.
4. Magenes G., Calvi G.M., 1997, "In-plane seismic response of brick masonry walls", Earthquake Engineering and Structural Dynamics, 26.
5. Galasco, A., Lagomarsino, S., Penna, A., 2002, TREMURI Program: Seismic Analyser of 3D Masonry Buildings, University of Genoa.
6. Galasco, A., Lagomarsino S., Penna, A., Resemini, S. "Non-linear seismic analysis of masonry structures", Proc. 13th WCEE, 2004, Vancouver, paper n.843.
7. Bonett R., Penna A., Lagomarsino S., Barbat A., Pujades L., Moreno R., 2003, Evaluación de la vulnerabilidad sísmica de estructuras de mampostería no reforzada. Aplicación a un edificio de la zona de l'Eixample en Barcelona (España). Revista Internacional de Ingeniería de estructuras. Escuela Politécnica del Ejército, Ecuador, 8, 2: 91-120.
8. STAC program. "Stochastic análisis computacional", International Center for Numerical Methods in Engineering (CIMNE), Barcelona, 2002.
9. Fajfar, P. "Capacity spectrum method based on inelastic demand spectra". Earthquake Engineering and Structural Dynamics 1999, 28: 979-993.
10. RISK-UE project. "An advanced approach to earthquake risk scenarios with application to different European towns", European Commission, contract EVK4-CT-2000-00014, 2001-2004.